Microscopic Spiral Waves Reveal Positive Feedback in Subcellular Calcium Signaling

Peter Lipp and Ernst Niggli
Department of Physiology, University of Bern, CH-3012 Bern, Switzerland

ABSTRACT The regenerative Ca^{2+}-induced Ca^{2+} release mechanism is an important amplifier of signal transduction in diverse cells. In heart muscle cells, this mechanism contributes to the Ca^{2+} transient activating the mechanical contraction, but it is also believed to drive Ca^{2+} waves propagating within the cytosol. We investigated the subcellular Ca^{2+} distribution in heart muscle cells during spontaneous Ca^{2+} release using laser scanning confocal microscopy with a ratiometric fluorescent indicator technique. Besides planar Ca^{2+} waves with linear propagation, sequences of confocal optical sections also revealed spiral Ca^{2+} waves spinning around a subcellular core at ~1 Hz. Although the Ca^{2+} spirals were continuous processes they frequently exhibited an apparently oscillatory output function into the elongated cell body. These oscillatory waves emanating from the spiral at regular intervals were formally considered to be short outer segments of the spiral but could not be distinguished from planar Ca^{2+} waves propagating along the longitudinal cell axis. The complex spatiotemporal pattern of spiral Ca^{2+} waves implies the participation of an active process exhibiting a large degree of positive feedback, most likely the Ca^{2+}-induced Ca^{2+} release mechanism.

INTRODUCTION

Numerous cells including hepatocytes (Woods et al., 1987; Somogyi and Stucki, 1991), astrocytes (Cornell-Bell et al., 1990), oocytes (Lechleiter et al., 1991), and several muscle cells (Näbauer et al., 1989; Niggli and Lederer, 1990*b*; Jacquemond et al., 1991; Blatter and Wier, 1992) use a Ca^{2+}-induced Ca^{2+} release mechanism for subcellular signaling. Generally, this mechanism is responsible for a transient or oscillatory Ca^{2+} release from intracellular stores (Dupont et al., 1991). In heart muscle electrical excitation is linked to mechanical contraction by means of Ca^{2+}-induced Ca^{2+} release (Fabiato, 1985), a hypothesis that is also supported by the observation of subcellular planar Ca^{2+} waves in isolated cardiac myocytes (Wier et al., 1987; Takamatsu and Wier, 1990; Williams et al., 1992). However, mathematical modeling of intracellular Ca^{2+} diffusion has indicated that the differences between planar waves propagating by simple diffusion and waves driven by a regenerative mechanism exhibiting positive feedback may be rather subtle (Blatter and Wier, 1992). In this paper we present complex patterns of Ca^{2+} wave propagation which clearly demonstrate that an active process is carrying the waves in cardiac myocytes.

MATERIALS AND METHODS

Cell preparation and solutions

Cardiac myocytes were isolated from adult guinea pigs by standard enzymatic procedures. Spontaneous Ca^{2+} release from the sarcoplasmic reticulum (SR) under conditions of Ca^{2+} overload was induced by raising free $[Ca^{2+}]$ in the extracellular solution (mM): NaCl, 145; KCl, 4; $CaCl_2$, 1 to 10; $MgCl_2$, 1; glucose, 10; HEPES/NaOH 10; pH 7.4, temperature 20–23°C.

Received for publication 21 June 1993 and in final form 30 August 1993.
Address reprint requests to Dr. Ernst Niggli, Department of Physiology, University of Bern, Bühlplatz 5, CH-3012 Bern, Switzerland.

0006-3495/93/12/2272/05 $2.00

Cells were loaded with a mixture of the two Ca^{2+} indicators Fluo-3 and Fura-Red (Molecular Probes, Eugene, OR) by exposure to 2 μM of each AM-ester for 15 min at 20°C. De-esterification of the fluorophores was allowed to proceed for at least 30 min.

Ca^{2+} measurements

Ratiometric confocal Ca^{2+} measurements were performed as described previously (Lipp and Niggli, 1993). Briefly, fluorescence emission from the two indicators Fluo-3 and Fura-Red was recorded simultaneously at up to 8 frames/s (192 × 96 pixels/channel) in the dual-emission mode of a MRC-600 laser-scanning confocal microscope (BioRad, Glattbrugg, Switzerland; objective lens: Zeiss Neofluar 63×, 1.25 numerical aperture). To maintain the fast scanning rate of the confocal microscope the images were recorded on videotape. The frames were digitized and corrected for nonlinearities of the video recorder off-line. The 514 nm line of the argon laser was used to excite both fluorophores while fluorescence was detected at 540 ± 15 nm (Fluo-3) and >600 nm (Fura-Red). Individual images of the sequences in Figs. 1 *A* and 3 *A* represent ratiometric fluorescence signals and were computed from confocal optical sections by dividing the Fluo-3 image by the Fura-Red image. Computed ratios were mapped linearly to correspond to the available 256 colors. Since these cells were loaded with the indicators by exposure to the AM-ester the extent of dye loading was not known to us. We therefore did not apply our in vitro calibration to the data. The background was covered manually by applying a black mask. Dicer (Spyglass, Campaign, IL) software running on a Macintosh IIcx computer (Apple, Walisellen, Switzerland) was used for the volume-rendering computations. Volume elements (voxels) with ratios above an arbitrarily chosen level (twofold resting) were considered to be opaque, while all others were treated as transparent. Each data cube contains data from 40 optical sections. To obtain an appropriate aspect ratio, 240 additional sections (6:1) were generated by linear interpolation along the vertical axis (= time).

RESULTS AND DISCUSSION

Fig. 1 *A* shows a sequence of confocal Ca^{2+} images recorded from a cardiac ventricular myocyte exhibiting spontaneous Ca^{2+} release from the SR. Spontaneous Ca^{2+} release was induced by overloading the cell with Ca^{2+}. Subcellular release events took place in the lower left end of the cell at intervals ranging from 1000 to 1800 ms. After a short period

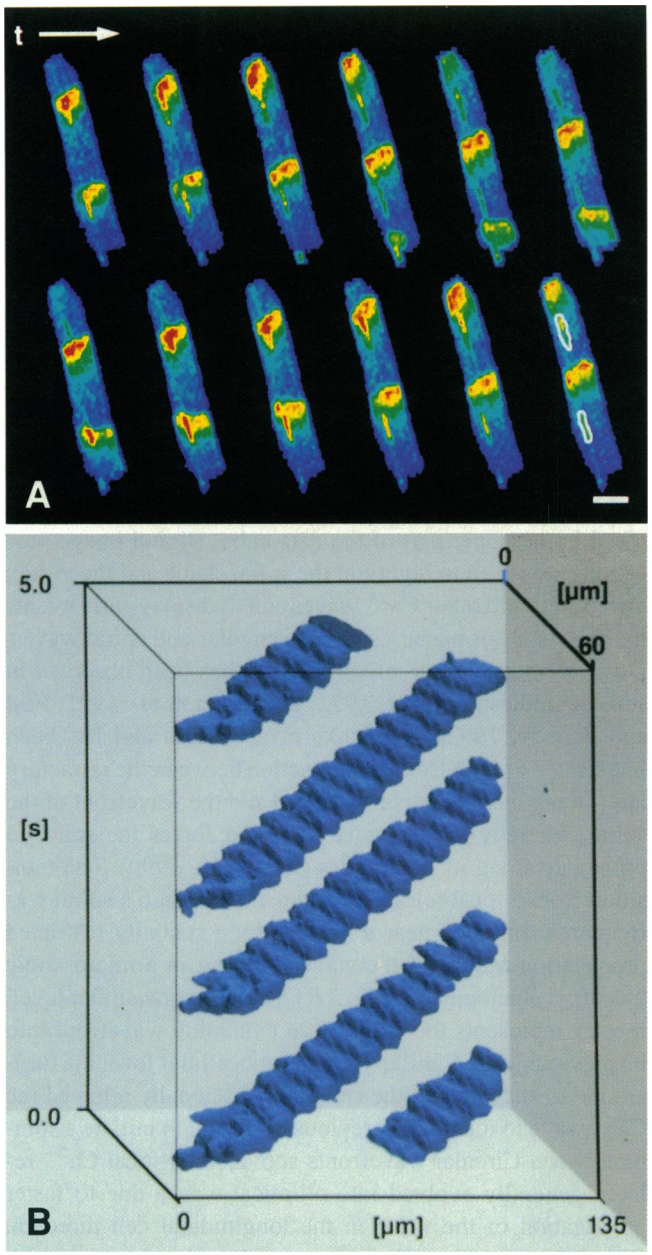

FIGURE 1 Planar Ca^{2+} waves imaged with confocal laser scanning microscopy. (*A*) A series of ratiometric confocal optical sections reveals planar Ca^{2+} waves traveling along the longitudinal axis of an isolated cardiac myocyte. Although the optical section is only about 0.7 μm thick, the spatial extension of the wave along the vertical axis of the cell ensures that the waves are at least partially in the focal plane and cannot intermittently escape confocal detection. Two nuclei displaying delayed Ca^{2+} signals are outlined in the last panel and can be recognized in most frames. Length of scale bar in all figures: 20 μm, frame interval 125 ms (from *left to right*; see *arrow*). (*B*) A sequence of 40 confocal images was converted into a pseudo-three-dimensional object by stacking the individual frames on top of each other. Volume-rendering software was used to visualize the planar waves of elevated Ca^{2+} as solid objects in space.

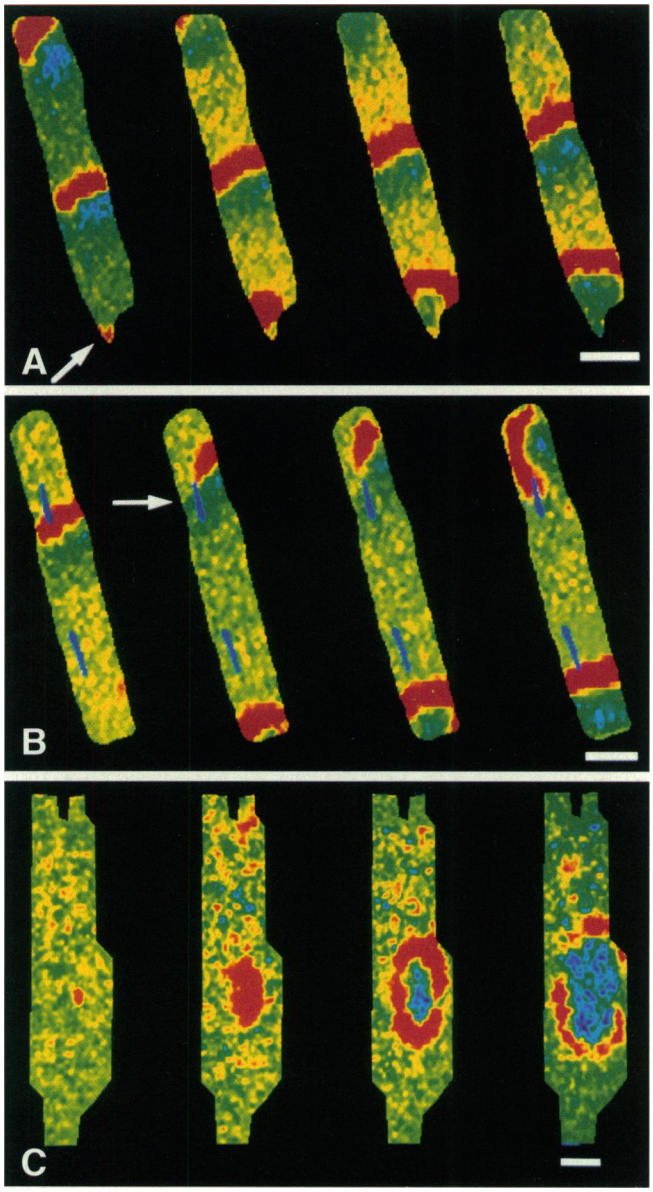

FIGURE 2 Early events in the genesis of planar, spiral, and circular waves. For these panels the contrast of the wavefront was enhanced by calculating differences between two consecutive ratio images. (*A*) Immediately after a spontaneous focal release (↓) the wavefront was noticeably circular and became apparently planar while propagating in the cell. (*B*) The "conduction block" near a nucleus (marked in blue) can favor the transition from a planar to a spiral wave by giving rise to a "micro-reentry" phenomenon. This sporadic unidirectional block of propagation (↓) suggests the existence of local and time-dependent variability in the positive feedback of the CICR. (*C*) A focal release near the center of a cell initiates a circular wave. More rapid propagation along the longitudinal cell axis results in an elliptical shape of the wavefront.

of propagation as a circular wave (Fig. 2*A*) each spontaneous release initiated a Ca^{2+} wave which traveled along the longitudinal cell axis as a planar wave, presumably driven by the Ca^{2+}-induced Ca^{2+} release (CICR) mechanism. The propagation velocity of the planar Ca^{2+} waves was 65 μm/s, rather slow for cardiac myocytes which were Ca^{2+} overloaded. In other studies propagation velocities between 90 μm/s and 100 μm/s have been described (Takamatsu and Wier, 1990; Takamatsu et al., 1991). Variations of intracellular indicator concentration or other experimental factors which influence the positive feedback in CICR may explain these differences.

The increase in local $[Ca^{2+}]$ was temporally and spatially transient because elevations of cytosolic $[Ca^{2+}]$ are generally terminated by Ca^{2+} re-sequestration into the SR via the Ca^{2+} pump and by Ca^{2+} extrusion via the Na-Ca exchange (Lipp and Pott, 1988; Niggli and Lederer, 1991). Therefore, the subcellular region of elevated $[Ca^{2+}]$ exhibited a finite length, which was ~10 μm in this cell. Because the time-varying topology of more complex waves is difficult to recognize from static image sequences, we transformed the time series of two-dimensional confocal sections into a pseudo-three-dimensional data cube where the vertical axis represents time advancing from bottom to top. This data representation is equivalent to the temporal stacks used by other authors, but here both spatial dimensions are retained (Lechleiter et al., 1991; Davidenko et al., 1992). Volume-rendering software was used to visualize the waves of elevated $[Ca^{2+}]$ as solid objects in space while all other cellular structures were made transparent (Fig. 1 *B*). Each wave can be identified as a blue rodlike structure spanning the volume of the pseudo-three-dimensional data space from the left to the right, the inclination of the rods is proportional to the propagation velocity of the Ca^{2+} waves.

Interestingly, we frequently observed dramatic deviations from the simple linear propagation pattern, particularly when the waves were slow and the wavelength was short. Under these conditions the Ca^{2+} waves have sufficient space to travel along a route different from a simple linear path, even in cells as small as heart muscle cells (Figs. 2 *B* and 3). Furthermore, the two nuclei usually present in ventricular cardiac myocytes represent subcellular structures which are responsible for additional complexity in the motion of Ca^{2+} waves. Nuclei of cardiac myocytes do not participate in the active propagation of Ca^{2+} waves and effectively represent obstacles. These obstacles can be traversed only slowly by passive diffusion of Ca^{2+} ions through pores located in the nuclear envelope (Niggli and Lederer, 1990*a*; Lipp and Niggli, 1993). The subcellular "conduction block" caused by the nuclei can lead to the generation of more complicated patterns of wave propagation. The nucleus itself does not produce the complex waves, however. The nuclei are only likely to initiate a differential curvature along the propagating wavefront. The relationship between the curvature and the velocity is then responsible for generating and maintaining the complex wave. Patterns such as circular and spiral waves around a subcellular core are only expected to exist when a regenerative process is driving the waves and provided there is room for a subcellular path length longer than the wavelength of the Ca^{2+} wave itself (Fast et al., 1990).

Complex patterns of Ca^{2+} wave propagation are shown as a series of ratiometric confocal optical sections in Fig. 3 *A*. Three important observations can be made in this figure: (i) in the lower third of the myocyte a wave of elevated Ca^{2+} repeatedly spins around a subcellular core associated with a nucleus; (ii) each revolution of the spiral wave gives rise to a planar wave which travels along the longitudinal cell axis; (iii) toward the end of the sequence a planar wave moves around the second nucleus (upper third of the cell) and returns on the other side of the cytosol, eventually colliding head-on with the next incoming planar wave. The collision results in annihilation of both waves and demonstrates the refractoriness of the CICR mechanism (see arrow). This refractoriness most likely results from an inhibition of the CICR mechanism and has also been observed in *Xenopus* oocytes exhibiting circular and spiral Ca^{2+} waves (Lechleiter et al., 1991).

Volume rendering revealed a corkscrew-like structure representing a spiral spinning around a subcellular core with a rotation period of around 1 s (Fig. 3 *D*). Planar waves originating from the spiral wave appear as straight blue rods emanating from the corkscrew and projecting toward the right at regular intervals. The final head-on collision of two planar Ca^{2+} waves traveling in opposite directions can be recognized in the upper part of the data cube. Digital image processing was used to highlight the spiral shape and the vortex drift of this and other Ca^{2+} waves and to display early events in the genesis of planar as well as circular and spiral waves. Drift or "meandering" of spiral cores has been observed in several studies (Winfree, 1972; Lechleiter et al., 1991; Fast and Pertsov, 1992; Davidenko et al., 1992) and has been interpreted to arise from an interaction between the refractory tail (or any other refractory region) and the wavefront of the spiral, whereby the unexcitable region forces the spiral to propagate along its boundaries (Fast et al., 1990). The transition from a focal release or a planar wave into a spiral was frequently initiated near a nucleus by a spatially restricted propagation failure of the wave resulting in a microscopic "reentry" phenomenon (Fig. 2 *B*). On the supracellular level, reentry represents the entry of an excitation wavefront into its previous path. Similarly, on the subcellular level the turnaround of the wave at the cell end occasionally allowed the Ca^{2+} wave to reenter its previous route and to initiate a spinning wave. Circular wavefronts activated by focal Ca^{2+} release generally evolved into elliptical waves due to faster propagation of the wave in the longitudinal cell direction (Fig. 2 *C*), a characteristic that may be related to the ultrastructure of the myocyte. Both features of wave propagation suggest the existence of subcellular inhomogeneities and anisotropy in the positive feedback of CICR, elementary properties which are relevant to our understanding of Ca^{2+} signaling in general and excitation-contraction coupling in particular (Niggli and Lederer, 1990*b*; O'Neill et al., 1990). Several results have indicated that the degree of positive feedback in CICR may be quite variable from cell to cell, depending on the experimental conditions (e.g., O'Neill et al., 1990). The present results suggest a variability of the positive feedback even on the subcellular level. This notion implies the existence of functionally separate SR elements exhibiting differences in gain (Niggli and Lederer, 1990*b*). The functional SR elements may correspond to the "cluster bombs" proposed in a mathematical model of cardiac excitation-contraction coupling (Stern, 1992).

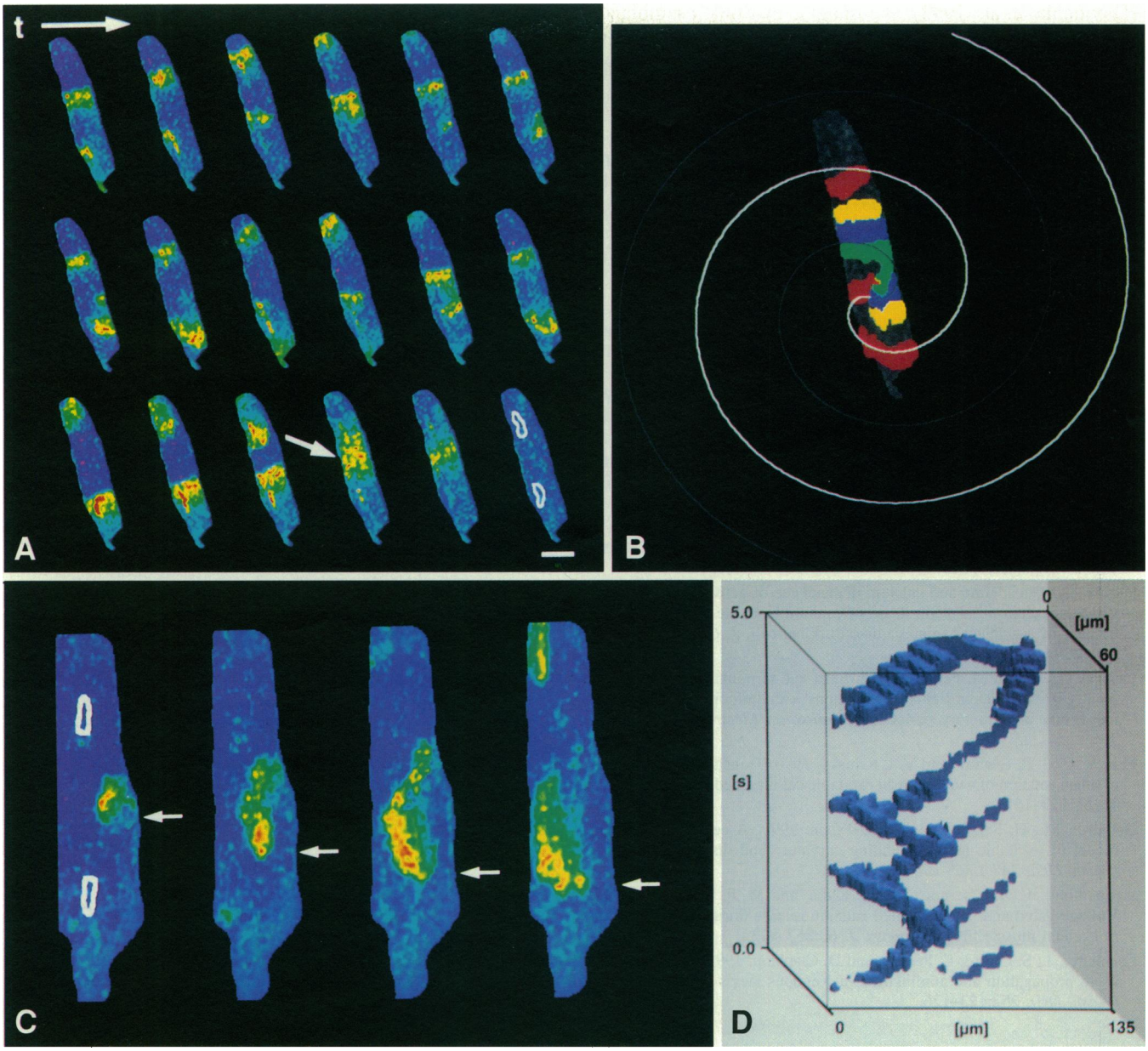

FIGURE 3 Spiral Ca^{2+} waves imaged with confocal laser scanning microscopy. (*A*) A sequence of ratio images reveals a spiral wave spinning around the lower nucleus and eliciting planar Ca^{2+} waves similar to those displayed in Fig. 1 *A*. The panels in the lowest row show a head-on collision of two planar waves traveling in opposite directions and resulting in annihilation of both waves (see arrow). Every second image of a series acquired at 125 ms intervals is shown, time runs from left to right. Scale bar: 20 µm. (*B*) Pseudo-colored density slices recorded at 125-ms intervals were superimposed on a gray-scale image of the resting cell. Two spirals are drawn beyond the cell boundaries to highlight the shape of the spiral wave. Since the no-flux boundary condition at the cell membrane does not affect the curvature of the spirals at the level of our observations, the planar waves may be considered as short cut-out segments of the original spiral wave. (*C*) The noticeable drift of the spiral core (←) suggests an interaction between the refractory tail and the wavefront of the spiral. (*D*) Volume rendering shows a corkscrew-like structure on the left and the collision of two planar waves near the top of the data cube. A vertical cross section through the same data cube was applied without performing volume rendering and reveals planar waves radiating from the spiral to the right.

The existence of waveforms as complex as spirals rules out the possibility that the Ca^{2+} waves frequently observed in cardiac myocytes are simply due to diffusion of released Ca^{2+} ions. Diffusion is an inherently random process and cannot change direction or travel along curved trajectories. Spatially complex propagation phenomena are predicted by mathematical models (Gerhardt et al., 1990; Fast et al., 1990) in a variety of systems exhibiting positive feedback (e.g., purely chemical reactions (Winfree, 1972) as well as biological processes (Lechleiter et al., 1991; Davidenko et al., 1992)). In heart muscle, regenerative processes like the conduction of electrical excitation have been reported to prevail as spiral waves on the macroscopic level, although on spatial and temporal scales different from the present observations

(Davidenko et al., 1992). We imagine that this resemblance is not coincidental but results from a fundamental similarity of spatially organized signal transduction networks exhibiting positive feedback and refractoriness.

We thank Drs. V. G. Fast, H-R. Lüscher, J. S. Shiner, and R. Weingart for discussions and comments on the manuscript. This work was supported by the Swiss National Science Foundation (31-28545.90 and 3100-037417.93) and by the M-E. Müller Foundation.

REFERENCES

Blatter, L. A., and W. G. Wier. 1992. Agonist-induced $[Ca^{2+}]_i$ waves and Ca^{2+}-induced Ca^{2+} release in mammalian vascular smooth muscle cells. *Am. J. Physiol.* 263:H576–H586.

Cornell-Bell, A. H., S. M. Finkbeiner, M. S. Cooper, and S. J. Smith. 1990. Glutamate induces calcium waves in cultured astrocytes: long-range glial signaling. *Science (Wash. DC).* 247:470–473.

Davidenko, J. M., A. V. Pertsov, R. Salomonsz, W. Baxter, and J. Jalife. 1992. Stationary and drifting spiral waves of excitation in isolated cardiac muscle. *Nature (Lond.).* 355:349–351.

Dupont, G., M. J. Berridge, and A. Goldbeter. 1991. Signal-induced Ca^{2+} oscillations—properties of a model based on Ca^{2+}-induced Ca^{2+} release. *Cell Calcium.* 12:73–85.

Fabiato, A. 1985. Time and calcium dependence of activation and inactivation of calcium-induced release of calcium from the sarcoplasmic reticulum of a skinned canine cardiac Purkinje cell. *J. Gen. Physiol.* 85: 247–289.

Fast, V. G., and A. M. Pertsov. 1992. Shift and termination of functional reentry in isolated ventricular preparations with quinidine-induced inhomogeneity in refractory period. *J. Cardiovasc. Electrophysiol.* 3:255–265.

Fast, V. G., I. R. Efimov, and V. I. Krinsky. 1990. Transition from circular to linear rotation of a vortex in an excitable cellular medium. *Physics Let. A* 151:157–161.

Gerhardt, M., H. Schuster, and J. J. Tyson. 1990. A cellular automaton model of excitable media including curvature and dispersion. *Science (Wash. DC).* 247:1563–1566.

Jacquemond, V., L. Csernoch, M. G. Klein, and M. F. Schneider. 1991. Voltage-gated and calcium-gated calcium release during depolarization of skeletal muscle fibers. *Biophys. J.* 60:867–873.

Lechleiter, J., S. Girard, E. Peralta, and D. Clapham. 1991. Spiral calcium wave propagation and annihilation in Xenopus laevis oocytes. *Science (Wash. DC).* 252:123–126.

Lipp, P., and E. Niggli. 1993. Ratiometric confocal Ca^{2+}-measurements with visible wavelength indicators in isolated cardiac myocytes. *Cell Calcium.* 14:359–372.

Lipp, P., and Pott, L. 1988. Voltage dependence of sodium-calcium exchange currents in guinea-pig atrial myocytes determined by means of an inhibitor. *J. Physiol. (Lond.).* 403:355–366.

Näbauer, M, G. Callewaert, L. Cleemann, and M. Morad. 1989. Regulation of calcium release is gated by calcium current, not gating charge, in cardiac myocytes. *Science (Wash. DC).* 244:800–803.

Niggli, E., and W. J. Lederer. 1990a. Real-time confocal microscopy and calcium measurements in heart muscle cells: towards the development of a fluorescence microscope with high temporal and spatial resolution. *Cell Calcium.* 11:121–130.

Niggli, E., and W. J. Lederer. 1990b. Voltage-independent calcium release in heart muscle. *Science (Wash. DC).* 250:565–568.

Niggli, E., and W. J. Lederer. 1991. Molecular operations of the Na-Ca exchanger revealed by conformation currents. *Nature (Lond.).* 349:621–624.

O'Neill, S. C., J. G. Mill, and D. A. Eisner. 1990. Local activation of contraction in isolated rat ventricular myocytes. *Am. J. Physiol.* 27:C1165-C1168.

Somogyi, R., and J. W. Stucki. 1991. Hormone-induced calcium oscillations in liver cells can be explained by a simple one pool model. *J. Biol. Chem.* 266:11068–11077.

Stern, M. D. 1992. Theory of excitation-contraction coupling in cardiac muscle. *Biophys. J.* 63:497–517.

Takamatsu, T., and W. G. Wier. 1990. Calcium waves in mammalian heart: quantification of origin, magnitude, waveform, and velocity. *FASEB J.* 4:1519–1525.

Takamatsu, T., T. Minamikawa, H. Kawachi, and S. Fujita. 1991. Imaging of calcium wave propagation in guinea-pig ventricular cell pairs by confocal laser scanning microscopy. *Cell Struc. Funct.* 16:341–346.

Wier, W. G., M. B. Cannell, J. R. Berlin, E. Marban, and W. J. Lederer. 1987. Cellular and subcellular heterogeneity of $[Ca^{2+}]_i$ in single heart cells revealed by fura-2. *Science (Wash. DC).* 235:325–328.

Williams, D. A., L. M. Delbridge, S. H. Cody, P. J. Harris, and T. O. Morgan. 1992. Spontaneous and propagated calcium release in isolated cardiac myocytes viewed by confocal microscopy. *Am. J. Physiol.* 262:C731-C742.

Winfree, A. T. 1972. Spiral waves of chemical activity. *Science (Wash. DC).* 175:634–636.

Woods, N. M., K. S. R. Cuthbertson, and P. H. Cobbold. 1987. Agonist induced oscillations in cytoplasmic free calcium concentration in single rat hepatocytes. *Cell Calcium.* 8:79–100.